

Simulation of detection and scattering of sound waves by the lateral line of a fish

V M Adamyan, I Y Popov, I V Blinova, and V V Zavalniuk

Citation: Chin. Phys. B, 2022, 31 (**2**): 024301. DOI: 10.1088/1674-1056/ac1b81
Journal homepage: http://cpb.iphy.ac.cn; http://iopscience.iop.org/cpb

What follows is a list of articles you may be interested in

Broadband topological valley-projected edge-states transport in composite structure phononic crystal

Hong-Yong Mao(毛鸿勇), Fu-Jia Chen(陈福家), Kai Guo(郭凯), and Zhong-Yi Guo(郭忠义)
Chin. Phys. B, 2021, 30 (**8**): 084302. DOI: 10.1088/1674-1056/abea89

Weak-focused acoustic vortex generated by a focused ring array of planar transducers and its application in large-scale rotational object manipulation

Yuzhi Li(李禹志), Peixia Li(李培霞), Ning Ding(丁宁), Gepu Guo(郭各朴), Qingyu Ma(马青玉), Juan Tu(屠娟), and Dong Zhang(章东)
Chin. Phys. B, 2021, 30 (**4**): 044302. DOI: 10.1088/1674-1056/abca1f

Axial acoustic radiation force on an elastic spherical shell near an impedance boundary for zero-order quasi-Bessel-Gauss beam

Yu-Chen Zang(臧雨宸), Wei-Jun Lin(林伟军), Chang Su(苏畅), and Peng-Fei Wu(吴鹏飞)
Chin. Phys. B, 2021, 30 (**4**): 044301. DOI: 10.1088/1674-1056/abca27

Radiation force and torque on a two-dimensional circular cross-section of a non-viscous eccentric layered compressible cylinder in acoustical standing waves

F G Mitri
Chin. Phys. B, 2021, 30 (**2**): 024302. DOI: 10.1088/1674-1056/abbbd9

Acoustic radiation force on thin elastic shells in liquid

Run-Yang Mo(莫润阳), Jing Hu(胡静), Shi Chen(陈时), Cheng-Hui Wang(王成会)
Chin. Phys. B, 2020, 29 (**9**): 094301. DOI: 10.1088/1674-1056/ab943e

---

Simulation of detection and scattering of sound waves by the lateral line of a fish

V M Adamyan[1], I Y Popov[2,†], I V Blinova[2], and V V Zavalniuk[1,3]

[1] *Odessa I.I. Mechnikov National University, Dvoryanskaya Str.* 2, *Odesa*, 65082, *Ukraine*
[2] *ITMO University, Kronverkskiy*, 49, *Saint Petersburg*, 197101, *Russia*
[3] *Odessa Military Academy*, 10 *Fontanska Road, Odesa* 65009, *Ukraine*

(Received 6 March 2021; revised manuscript received 12 July 2021; accepted manuscript online 7 August 2021)

A solvable model of lateral line of a fish based on a wave equation with additional boundary conditions on a set of isolated points is proposed. Within the framework of this model it is shown that the ratio of pressures on lateral lines on different fish flanks, as well as the cross section of sound scattering on both the lines, strongly depends on angles of incidence of incoming sound waves. The strong angular dependence of the pressure ratio seems to be sufficient for the fish to determine the directions from which the sound is coming.

Keywords: acoustic equation, point self-adjoint perturbations of Laplace operator, scattering, lateral line

PACS: 43.20.Fn, 02.30.Tb **DOI:** 10.1088/1674-1056/ac1b81

1. Introduction

Sound detection capabilities of fishes are mainly based on two sensory systems, the inner ears and small receptor organs called "neuromasts" with sizes in order of 100 μm; in some fish species a gas filled swim bladder is also involved in sound detection.[1,2] There are two types of neuromasts, i.e., superficial and canal. Superficial neuromasts are scattered on surface of a fish and mainly responsible for detection of surrounding flows, while the canal neuromasts are found in special subdermal canals and percept a pressure gradient of the flow.[3–6] It was shown that fishes are able to localize the direction to the sound source and that the amount of data gathered by the auditory organs is quite sufficient for some species to navigate and hunt in complex dark environments.[7–11] However, full understanding of exact mechanisms of fish sound-based navigation and the details of interactions between fish auditory systems have not been achieved yet.

Sound perception is a multi-stage event that requires four components to occur: a source of vibration, a transmitting medium, a receiving detector, and an interpreting nervous system. Sound energy is carried by motion of the particles that make up the transmitting medium. For inhabitants of aquatic environment, the carrier of sound is water in which they are located. Most fish species and amphibians, among other natural tools, have a special organ known as the lateral line that detects and interprets water vibrations. Visually, as a rule, it represents two dark or light stripes, one on each side of the body trunk of the fish, stretching from the head to the end of the caudal peduncle. In fact, each of the stripes is a single fluid-filled longitudinal canal buried in the skin which contains arrays of equidistant neuromasts (this structure is shown in Fig. 1). The canal is connected to the external environment via secondary fluid-filled tubules that branch off from the main tube and penetrate the skin at regular intervals. Water vibrations are transmitted from the secondary tubules to the canal by sequential compression and expansion of fluid. These vibrations then jiggle the gelatinous domes of hair cells lining the canal. The neuromasts usually alternate with external openings of the canal.

Various aspects of fish hearing (acoustical parameters of lateral line and swim bladder, description of sound receiver, etc.) are described in Refs. [12–19].

In Refs. [20,21] a physical explanation (based on the resonance scattering of incoming sound wave) is given for a mechanism of the detection of a sound source by means of the lateral line organ. In a few words, a system of neuromasts can be approximately considered as a periodic system of identical acoustic resonators with small opening. It was shown that a monochromatic wave falling on such a system can excite edge waves in the vicinity of resonators. The intensity of such a wave drastically depends on the angle between the directions of the incident wave and the lateral line. The fish picks up incoming waves (through neuromasts due to pressure surges) and tunes in to them, changing the orientation of their body in order to achieve the maximum tactile sensation, and thus somehow determines the direction to the sound source.

In this paper, using these considerations as a starting point, we develop a simplified solvable model of the acoustic field in the vicinity of the lateral line, which allows us to compare the overpressure on opposite sides of the fish caused by a distant sound source and to describe the angular distribution of the resulting scattered sound waves.

†Corresponding author. E-mail: popov1955@gmail.com

© 2022 Chinese Physical Society and IOP Publishing Ltd

The proposed approach is based on the perturbation theory for the wave equation in the form of the system of additional boundary conditions at the points of location of neuromasts. In other words, we model the influence of the lateral line on the wave field in the immediate vicinity of the line as a perturbation induced by a system of identical zero-radius potentials[22] sitting in the places of neuromasts. In this way, one can easily supplement recent studies,[23–28] which have used physical instrumentation and mathematical modeling to show that the lateral line of fish is a subtle analyzer of the gradients of the surrounding hydrodynamic fields.

In Section 2, we briefly outline the proposed model and find the explicit expression of Green's function for the associated Helmholtz equation. Using the obtained expression for Green's function, in Section 3 we calculate the pressure on each neuromast in the field of a plane monochromatic wave. Meanwhile, considering the neuromasts of the lateral line as a scattering system, we determine the scattering amplitude of a plane monochromatic sound wave incident on this system at an arbitrary angle. Finally, in Section 4, the results obtained are illustrated by calculations based on them, which show that at certain not very low frequencies the ratio of pressures on mirror-symmetric neuromasts from both sides of the fish body, due to phase delay, can vary by many orders of magnitude, depending on the direction of the sound source and the body orientation of the fish. In this case, the resonance dependence of the total and differential scattering cross sections on the incidence angle of the incoming plane monochromatic wave and the orientation of the fish body is also manifested.

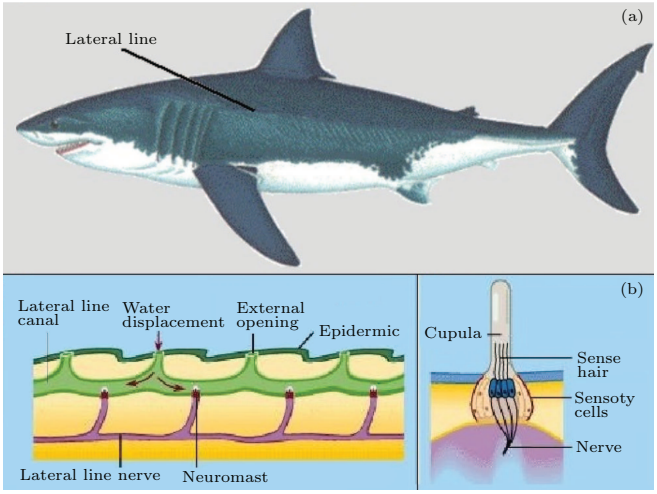


Fig. 1. The structure of the lateral line: (a) lateral line position, (b) lateral line structure, (c) neuromast structure.

2. Model description and Green's function

To construct a model to be solved, we replace small resonators (neuromasts) with point potentials and consider two parallel periodic chains of such potentials as a model of lateral lines on the sides of a fish. The mathematical basis for the development of such models is the theory of extensions of selfadjoint operators (see, e.g., Refs. [22,29–33]).

To explain the concept of an extension, let us consider the wave equation

$$\frac{\partial^2 \psi}{\partial t^2} = A\psi \tag{1}$$

for the velocity potential $\psi(\boldsymbol{r},t)$. Here, A is the Laplace differential operator $-c^2\Delta$ and c is the speed of sound. To add correctly a single zero-range potential located at the point $\boldsymbol{r}_0$ into Eq. (1) one can start from the standard defined self-adjoint Laplace operator $-c^2\Delta$ in $L_2(\mathbb{R}^3)$ with the domain $H^2(\mathbb{R}^3)$, where H^2 is the Sobolev space W_2^2 and we restrict this operator on the set of smooth functions vanishing together with its derivatives at the point $\boldsymbol{r}_0 = 0$. The closure of this restricted operator is a symmetric operator A_0 with the deficiency indices (1,1). The domain of the corresponding adjoint operator A_0^* consists, for any fixed $s = \sqrt{q^2 + \mathrm{i}\varepsilon}$, $\varepsilon \geq 0$, $\mathrm{Im}s > 0$, of all the functions in the form of sum

$$\psi(\boldsymbol{r}) = \psi_0(\boldsymbol{r}) + C_0^{\psi} \frac{\mathrm{e}^{\mathrm{i}s|\boldsymbol{r}|}}{4\pi|\boldsymbol{r}|},$$

where $\psi_0 \in H^2(\mathbb{R}^3)$, and C_0^{ψ} is any complex number. The boundary form for any ψ, υ from the domain of A_0^* admits the representation

$$(A^*\psi, \upsilon) - (\psi, A^*\upsilon) = \psi_0(0)\overline{C_0^{\upsilon}} - \overline{\upsilon_0(0)}C_0^{\psi}.$$

All selfadjoint extensions of A_0 are minimal restrictions of A_0^* on linear subsets of functions from the domain of A_0^*, for which the above boundary form equals zero. Each such restriction has the form of an additional linear relation

$$\psi_0(0) = \beta \cdot C_0^{\psi}, \quad \mathrm{Im}\beta = 0, \tag{2}$$

with a certain real parameter β, $-\infty < \beta \leq \infty$, which is superimposed on the functions from the domain of A_0^*.

The linear relation (2) takes the form of a boundary condition at the origin:

$$\lim_{|\boldsymbol{r}|\to 0} \left[\frac{\partial}{\partial|\boldsymbol{r}|} - \beta\right] |\boldsymbol{r}|\Psi = 0. \tag{3}$$

It is worth mentioning that the indicated self-adjoint operators, which are formally defined as Laplace differential operators on the set of functions satisfying the boundary condition (3), in three-dimensional problems legalize the heuristic expressions (see Ref. [22])

$$-c^2\Delta + \frac{1}{4\pi\beta}\delta(\boldsymbol{r}).$$

From now on we will assume that $\beta \geq 0$, since the selfadjoint extensions of A_0 related to the acoustic problems should be non-negative operators.

Further, for simplicity, we will neglect the curvature of the lateral canals on the sides of the fish, and as a model of these canals, together with their openings and neuromasts, we

will consider two parallel chains of equal equidistant potentials of zero radius of the form (3) with the distance between the nearest neighbors in each of the chains equal to a. We will assume that the second chain is shifted relative to the first by the vector $\boldsymbol{g} = g_1\boldsymbol{e}_1 + g_2\boldsymbol{e}_2$, where $\boldsymbol{e}_1$ and $\boldsymbol{e}_2$ are unit vectors along the axes X and Y, respectively, and that the indicated zero-range potentials are located along the first and second chains at points $\boldsymbol{r}_n^{(1)} = n\boldsymbol{a} = na\boldsymbol{e}_1$ and $\boldsymbol{r}_n^{(2)} = n\boldsymbol{a} + \boldsymbol{g}$, $n = 0, \pm1, \pm2, \ldots, \pm[N/2]$ (Fig. 2). Here Na is the length of each chain and $[x]$ is the integer part of x. Accepting that the length of the fish body trunk is much greater than the distance between the nearest canal neuromasts and for many fish species N reaches and even exceeds 100,[34] in what follows we will assume that $N \gg 1$. It worth mentioning that results of calculations using deduced below explicit asymptotic expression and corresponding numerical calculation cease to differ significantly for $N \geq 100$.

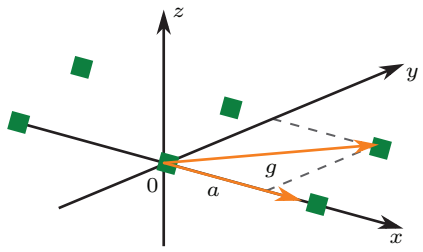


Fig. 2. Schematic of the model setup. Neuromasts (green squares) of the lateral line are on both sides of the fish's body.

As in the previous case, starting from the selfadjoint Laplacian in $L_2(\mathbb{R}^3)$ with the domain $H^2(\mathbb{R}^3)$, one can restrict this operator on the set of smooth functions vanishing at the indicated points of two chains. The closure of this restricted operator is a symmetric operator with infinite deficiency indices. It has rich family of self-adjoint extensions. To construct a suitable self-adjoint extension, one can take the corresponding adjoint operator. An element from its domain has the following form:

$$\begin{aligned}\psi(\boldsymbol{r}) \;=\; & \psi_0(x) + \sum_n \left\{ C_n^{(1)} \frac{\exp\left[\mathrm{i}s\,|\boldsymbol{r} - n\boldsymbol{a}|\right]}{|\boldsymbol{r} - n\boldsymbol{a}|} \right. \\ & \left. + C_n^{(2)} \frac{\exp\left[\mathrm{i}s\,|\boldsymbol{r} - n\boldsymbol{a} - \boldsymbol{g}|\right]}{|\boldsymbol{r} - n\boldsymbol{a} - \boldsymbol{g}|} \right\}, \end{aligned} \tag{4}$$

where ψ_0 belongs to the domain of the initial selfadjoint Laplacian, $C_n^{(1)}$ and $C_n^{(2)}$ are some constants, such that the series (4) converges to a $L_2(\mathbb{R}^3)$ function and $\mathrm{Im}s > 0$. Choosing the extension corresponding to the sum of the same zero-range potentials, as described above, at points $n\boldsymbol{a}$, $n\boldsymbol{a} + \boldsymbol{g}$, $n = 0, \pm1, \pm2, \ldots$, that is, the extension determined by the boundary conditions

$$\begin{aligned} & \lim_{\rho_n^\nu \to 0} \left[\frac{\partial}{\partial \rho_n^\nu} - \beta \right] \psi = 0, \quad \nu = 1, 2, \\ & \rho_n^1 = |\boldsymbol{r} - n\boldsymbol{a}|, \quad \rho_n^2 = |\boldsymbol{r} - n\boldsymbol{a} - \boldsymbol{g}|, \end{aligned} \tag{5}$$

yields a self-adjoint operator A, as required for the model in question. For simplicity, we set further $\boldsymbol{g} = g\boldsymbol{e}_2$.

Green's function for A (the kernel of the integral operator $\left(A - s^2 \cdot I\right)^{-1}$, $\mathrm{Im}s > 0$, I-unity operator) in general has the form

$$\begin{aligned} G\left(\boldsymbol{r}, \boldsymbol{r}', s\right) \;=\; & \frac{1}{4\pi} \frac{\exp\left[\mathrm{i}s\,|\boldsymbol{r} - \boldsymbol{r}'|\right]}{|\boldsymbol{r} - \boldsymbol{r}'|} \\ & + \sum_n \left\{ C_n^{(1)} \frac{\exp\left[\mathrm{i}s\,|\boldsymbol{r} - n\boldsymbol{a}|\right]}{|\boldsymbol{r} - n\boldsymbol{a}|} \right. \\ & \left. + C_n^{(2)} \frac{\exp\left[\mathrm{i}s\,|\boldsymbol{r} - n\boldsymbol{a} - \boldsymbol{g}|\right]}{|\boldsymbol{r} - n\boldsymbol{a} - \boldsymbol{g}|} \right\}. \end{aligned} \tag{6}$$

The system of boundary conditions (5) gives us a sufficient number of equations to uniquely determine the numerical values of the coefficients $C_n^{(1)}$, $C_n^{(2)}$. At the same time for $N \gg 1$, repeating the same considerations that are used in solid state theory to describe vibrational or electronic excitations of crystal structures, one can easily obtain approximate expressions for the same coefficients, the more accurate the more N. To obtain in this way an explicit expression for Green's function $G\left(\boldsymbol{r}, \boldsymbol{r}', s\right)$ we put

$$\begin{aligned} & \xi_k^{(j)} = \sum_n C_n^{(j)} \mathrm{e}^{\mathrm{i}kna}; \quad j = 1, 2, \quad -\frac{\pi}{a} \leq k < \frac{\pi}{a}, \\ & \chi_k^{(1)}(\boldsymbol{r}, s) = -\frac{1}{4\pi} \sum_n \frac{\exp\left[\mathrm{i}s\,|\boldsymbol{r} - n\boldsymbol{a}| + \mathrm{i}kna\right]}{|\boldsymbol{r} - n\boldsymbol{a}|}, \\ & \chi_k^{(2)}(\boldsymbol{r}, s) = -\frac{1}{4\pi} \sum_n \frac{\exp\left[\mathrm{i}s\,|\boldsymbol{r} - \boldsymbol{g} - n\boldsymbol{a}| + \mathrm{i}kna\right]}{|\boldsymbol{r} - \boldsymbol{g} - n\boldsymbol{a}|}, \\ & D(k, s) = \sum_{n \neq 0} \frac{\exp\left[\mathrm{i}s\,|n|\,a + \mathrm{i}kna\right]}{|n|\,a} + \mathrm{i}s - \beta, \\ & Q(k, s) = \sum_n \frac{\exp\left[\mathrm{i}s\,|n\boldsymbol{a} - \boldsymbol{g}| + \mathrm{i}kna\right]}{|n\boldsymbol{a} - \boldsymbol{g}|}. \end{aligned} \tag{7}$$

Using the boundary conditions (5) one can easily check that the functions $\xi_k^{(1)}, \xi_k^{(2)}$ satisfy the following system of algebraic equations:

$$\begin{aligned} & D(k, s)\,\xi_k^{(1)} + Q(k, s)\,\xi_k^{(2)} = \chi_k^{(1)}\left(\boldsymbol{r}', s\right), \\ & Q(-k, s)\,\xi_k^{(1)} + D(k, s)\,\xi_k^{(2)} = \chi_k^{(2)}\left(\boldsymbol{r}', s\right). \end{aligned} \tag{8}$$

Taking into account expressions (7), Eq. (8) and the inversion formula yields

$$C_n^{(j)} = \frac{a}{2\pi} \int_{-\frac{\pi}{a}}^{\frac{\pi}{a}} \mathrm{e}^{-\mathrm{i}ka} \xi_k^{(j)}\, \mathrm{d}k. \tag{9}$$

We can conclude that the following version of Krein's formula for Green's function for A is valid:

$$\begin{aligned} G\left(\boldsymbol{r}, \boldsymbol{r}', s^2\right) = & \frac{1}{4\pi} \frac{\exp\left[is\,|\boldsymbol{r} - \boldsymbol{r}'|\right]}{|\boldsymbol{r} - \boldsymbol{r}'|} \\ & - \frac{a}{2\pi} \int_{-\frac{\pi}{a}}^{\frac{\pi}{a}} \sum_{j,j'=1}^{2} \gamma_{jj'}(k) \chi_k^{(j)}(\boldsymbol{r}, s)\, \chi_{-k}^{(j')}\left(\boldsymbol{r}', s\right) \mathrm{d}k, \end{aligned}$$

$$\gamma_{11}(k,s)=\gamma_{22}(k,s)=\frac{D(k,s)}{W(k,s)},$$
$$\gamma_{12}(k,s)=\gamma_{21}(-k,s)=-\frac{Q(k,s)}{W(k,s)},$$
$$W(k,s)=D^2(k,s)-Q(-k,s)Q(k,s). \tag{10}$$

3. Remote source detection and sound scattering

If the complex amplitude of steady-state sound vibrations caused by a point source

$$A_+\delta(\boldsymbol{r}-\boldsymbol{R})\,\mathrm{e}^{-\mathrm{i}\omega t},$$

at a point $\boldsymbol{R}$ creates an excess variable pressure $p_0\,\mathrm{e}^{-\mathrm{i}\omega t}$ at a short distance r_0, $qr_0\ll 1$ from the source, then at arbitrary point $\boldsymbol{r}$ the complex amplitude of the excess pressure $p(\boldsymbol{r})\,\mathrm{e}^{-\mathrm{i}\omega t}$ will be determined by the expression

$$p(\boldsymbol{r})=4\pi r_0 p_0 G\left(\boldsymbol{r},\boldsymbol{R},q^2+\mathrm{i}0\right). \tag{11}$$

From now on we will assume that the distance from the origin to the remote source reads $|\boldsymbol{R}|=R\gg Na$.

Within the framework of the model under consideration, the expression (11) is singular at the points mimicking neuromasts' positions on the lateral line. To get around this difficulty, assuming that r_0 in (11) is significantly smaller than a, we will define the pressure at points $\boldsymbol{r}_n^{(1)}=n\boldsymbol{a},\boldsymbol{r}_n^{(2)}=n\boldsymbol{a}+\boldsymbol{g}$, $n=0,\pm1,\pm2,\ldots$ as the average

$$p\left(\boldsymbol{r}_n^{(j)},t\right)=\frac{3}{4\pi r_0^3}\int_{|\boldsymbol{r}-\boldsymbol{r}_n^{(j)}|<r_0}p(\boldsymbol{r},t)\,\mathrm{d}\boldsymbol{r},\quad j=1,2. \tag{12}$$

Krein's formula (10) and explicit expressions (7) and (8) for its entries yield

$$p\left(\boldsymbol{r}_n^{(l)},t\right)\underset{r_0\to0}{=}-\frac{3p_0a}{4\pi}\int_{-\frac{\pi}{a}}^{\frac{\pi}{a}}\sum_{j=1}^{2}\gamma_{lj}(k)\chi_{-k}^{(j)}\left(\boldsymbol{r}',s\right)\mathrm{d}k\cdot\mathrm{e}^{-\mathrm{i}\omega t},$$
$$l=1,2. \tag{13}$$

Taking into account that the sound absorption in water increases with frequency, we restrict ourselves also to cases in which the frequency of incoming sound satisfies the condition

$$\omega<\frac{\pi c}{a}. \tag{14}$$

Remember that

$$\lim_{r\to\infty}\lim_{\varepsilon\downarrow0}\frac{1}{4\pi}\frac{\exp\left[\mathrm{i}s|\boldsymbol{r}-\boldsymbol{R}|\right]}{|\boldsymbol{r}-\boldsymbol{R}|}=\frac{1}{4\pi}\frac{\mathrm{e}^{\mathrm{i}qR}}{R}\,\mathrm{e}^{-\mathrm{i}q(\boldsymbol{b}\cdot\boldsymbol{r})}+O\left(\frac{1}{R^2}\right),$$
$$s^2=\frac{\omega^2}{c^2}+\mathrm{i}\varepsilon\equiv q^2+\mathrm{i}\varepsilon,$$
$$\boldsymbol{b}=\frac{1}{R}\cdot\boldsymbol{R}=(\cos\theta_X,\sin\theta_X\sin\varphi,\cos\theta_X\cos\varphi), \tag{15}$$

where θ_X and φ are polar and azimuthal angles, respectively (see Fig. 3), and

$$\frac{a}{2\pi}\sum_{n=-N}^{N}\mathrm{e}^{\mathrm{i}(ka-k'a)n}\underset{N\to\infty}{\approx}\sum_{l=-\infty}^{\infty}\delta(ka-k'a+2\pi l). \tag{16}$$

The expressions for excess pressures $P^{(1)}(t)$ and $P^{(2)}(t)$ on two parallel parts of the lateral line can be deduced from Eq. (13) with the account of the asymptotic expression (15), formula (16) and the restriction (13). Assuming that $R\gg L$, i.e., the distance between the fish and a remote point source significantly exceeds the length of the lateral line, the expressions for $P^{(1)}(t)$, $P^{(2)}(t)$ can be written in the following form:

$$P^{(1)}(t)=-\frac{3p_0}{2R}\,\mathrm{e}^{\mathrm{i}(qR-\omega t)}\left[\frac{1-\mathrm{e}^{-\mathrm{i}q(\boldsymbol{d}\cdot\boldsymbol{g})}}{D(q\cos\theta_X,q^2+\mathrm{i}0)-Q(q\cos\theta_X,q^2+\mathrm{i}0)}+\frac{1+\mathrm{e}^{-\mathrm{i}q(\boldsymbol{d}\cdot\boldsymbol{g})}}{D(q\cos\theta_X,q^2+\mathrm{i}0)+Q(q\cos\theta_X,q^2+\mathrm{i}0)}\right],$$
$$P^{(2)}(t)=-\frac{3p_0}{2R}\,\mathrm{e}^{\mathrm{i}(qR-\omega t)}\left[\frac{1-\mathrm{e}^{-\mathrm{i}q(\boldsymbol{d}\cdot\boldsymbol{g})}}{D(q\cos\theta_X,q^2+\mathrm{i}0)-Q(q\cos\theta_X,q^2+\mathrm{i}0)}-\frac{1+\mathrm{e}^{-\mathrm{i}q(\boldsymbol{d}\cdot\boldsymbol{g})}}{D(q\cos\theta_X,q^2+\mathrm{i}0)+Q(q\cos\theta_X,q^2+\mathrm{i}0)}\right]. \tag{17}$$

These expressions make it possible in principle to determine the direction of the radius vector drawn from the fish to a remote source.

For the scattering of a plane sound wave

$$\psi_0(\boldsymbol{r},t)=\exp\mathrm{i}\left[(\boldsymbol{q}\cdot\boldsymbol{r})-\omega t\right],$$
$$\boldsymbol{q}=q\boldsymbol{b}\equiv\frac{\omega}{c}\boldsymbol{b},\quad\boldsymbol{b}=(\cos\theta_X,\cos\theta_Y,\cos\theta_Z) \tag{18}$$

by the considered system of point potentials the corresponding solution of the wave equation (1) is determined according to the Lippmann–Schwinger equation

$$\psi(\boldsymbol{r},t)=\mathrm{e}^{-\mathrm{i}\omega t}\lim_{\varepsilon\downarrow0}-\mathrm{i}\varepsilon\int_{\mathbb{R}^3}G\left(\boldsymbol{r},\boldsymbol{r}',q^2+\mathrm{i}\varepsilon\right)\mathrm{e}^{\mathrm{i}q\boldsymbol{r}'}\,\mathrm{d}\boldsymbol{r}', \tag{19}$$

(details can be found in Ref. [35]).

Note that

$$\lim_{\varepsilon\downarrow0}\frac{-\mathrm{i}\varepsilon}{4\pi}\int_{\mathbb{R}^3}\frac{\exp\left[\mathrm{i}s|\boldsymbol{r}-\boldsymbol{r}'|\right]}{|\boldsymbol{r}-\boldsymbol{r}'|}\,\mathrm{e}^{\mathrm{i}q(\boldsymbol{b}\cdot\boldsymbol{r}')}\,\mathrm{d}\boldsymbol{r}'=\mathrm{e}^{\mathrm{i}q(\boldsymbol{b}\cdot\boldsymbol{r})},$$
$$s=\sqrt{q^2+\mathrm{i}\varepsilon},\quad|\boldsymbol{b}|=1. \tag{20}$$

Therefore, referring to the functions in (7), in the limit $N\to\infty$ we have

$$\lim_{\varepsilon\downarrow0}-\mathrm{i}\varepsilon\int_{\mathbb{R}^3}\chi_k^{(1)}\left(\boldsymbol{r}',s\right)\mathrm{e}^{\mathrm{i}q(\boldsymbol{b}\cdot\boldsymbol{r}')}\,\mathrm{d}\boldsymbol{r}'$$
$$=\frac{2\pi}{a}\sum_{l=-\infty}^{\infty}\delta\left(k-\frac{2\pi l}{a}-qb_X\right),$$

$$\lim_{\varepsilon\downarrow 0} -\mathrm{i}\varepsilon \int_{\mathbb{R}^3} \chi_k^{(2)}(\boldsymbol{r}',s)\, \mathrm{e}^{\mathrm{i}q(\boldsymbol{b}\cdot\boldsymbol{r}')}\,\mathrm{d}\boldsymbol{r}' = \mathrm{e}^{\mathrm{i}q(\boldsymbol{b}\cdot\boldsymbol{g})}\frac{2\pi}{a}\sum_{l=-\infty}^{\infty}\delta\left(k-\frac{2\pi l}{a}-qb_X\right). \tag{21}$$

Hence, by virtue of Eqs. (10) and (19)–(21) we have

$$\begin{aligned}
&\mathrm{e}^{\mathrm{i}\omega t}\psi(\boldsymbol{r},t) - \mathrm{e}^{\mathrm{i}(\boldsymbol{q}\cdot\boldsymbol{r})} \\
&= -\sum_{l=-\infty}^{\infty}\left\{\left[\gamma_{11}\left(qb_X+\frac{2\pi l}{a}\right)+\gamma_{12}\left(qb_X+\frac{2\pi l}{a}\right)\mathrm{e}^{-\mathrm{i}(\boldsymbol{q}\cdot\boldsymbol{g})}\right]\right. \\
&\times\chi^{(1)}_{qb_X+\frac{2\pi l}{a}}(\boldsymbol{r},s) \\
&+\left[\gamma_{21}\left(qb_X+\frac{2\pi l}{a}\right)+\gamma_{22}\left(qb_X+\frac{2\pi l}{a}\right)\mathrm{e}^{-\mathrm{i}(\boldsymbol{q}\cdot\boldsymbol{g})}\right] \\
&\left.\times\chi^{(2)}_{qb_X+\frac{2\pi l}{a}}(\boldsymbol{r},s)\right\}.
\end{aligned} \tag{22}$$

Remembering again the asymptotic expression (15) we also see that

$$\begin{aligned}
&\lim_{r\to\infty}\lim_{\varepsilon\downarrow 0}\chi_k^{(1)}(\boldsymbol{r},s) \\
&= \frac{1}{2a}\frac{\mathrm{e}^{\mathrm{i}qr}}{r}\sum_{l=-\infty}^{\infty}\delta\left(k-q\cos\vartheta_X-\frac{2\pi l}{a}\right), \\
&\lim_{r\to\infty}\lim_{\varepsilon\downarrow 0}\chi_k^{(2)}(\boldsymbol{r},s) \\
&= \frac{1}{2a}\frac{\mathrm{e}^{\mathrm{i}qr}}{r}\cdot\mathrm{e}^{-\mathrm{i}q(\boldsymbol{d}\cdot\boldsymbol{g})}\sum_{l=-\infty}^{\infty}\delta\left(k-q\cos\vartheta_X-\frac{2\pi l}{a}\right), \\
&\boldsymbol{d}=\frac{1}{r}\boldsymbol{r}.
\end{aligned} \tag{23}$$

Using relations (22) and (23) we find that the scattering amplitude $f_\omega(\boldsymbol{d},\boldsymbol{b})$,

$$\mathrm{e}^{\mathrm{i}\omega t}\psi(\boldsymbol{r},t) \underset{r\to\infty}{=} \mathrm{e}^{\mathrm{i}(\boldsymbol{q}\cdot\boldsymbol{r})} + f_\omega(\boldsymbol{d},\boldsymbol{b})\frac{\mathrm{e}^{\mathrm{i}qr}}{r}+O\left(\frac{1}{r^2}\right),$$

for $N\gg 1$ has the form

$$\begin{aligned}
f_\omega(\boldsymbol{d},\boldsymbol{b}) = -\sum_{l,l'=-\infty}^{\infty}\frac{1}{2a}&\left[\gamma_{11}\left(qb_X+\frac{2\pi l}{a}\right)\right. \\
&+\gamma_{12}\left(qb_X+\frac{2\pi l}{a}\right)\mathrm{e}^{-\mathrm{i}(\boldsymbol{q}\cdot\boldsymbol{g})} \\
&+\gamma_{21}\left(qb_X+\frac{2\pi l}{a}\right)\mathrm{e}^{\mathrm{i}(\boldsymbol{q}\cdot\boldsymbol{g})} \\
&\left.+\gamma_{22}\left(qb_X+\frac{2\pi l}{a}\right)\mathrm{e}^{-\mathrm{i}(\boldsymbol{q}\cdot\boldsymbol{g})}\right] \\
&\times\delta\left(q[b_X-d_X]-\frac{2\pi}{a}[l-l']\right) \\
&\times\eta_{[-\frac{\pi}{a},\frac{\pi}{a}]}\left(qb_X+\frac{2\pi l}{a}\right),
\end{aligned}$$

$$\eta_{[\alpha_1,\alpha_2]}(x) = \begin{cases} 1, & x\in[\alpha_1,\alpha_2], \\ 0, & x\notin[\alpha_1,\alpha_2]. \end{cases} \tag{24}$$

As followed from (24), scattering from the lateral line can be observed only when the projections of the wave vectors of the waves incident on this line and reflected from it satisfy the Bragg-type condition

$$q(\cos\theta_X-\cos\vartheta_X)=\frac{2\pi}{a}l,\quad l=0,\pm1,\pm2,\ldots. \tag{25}$$

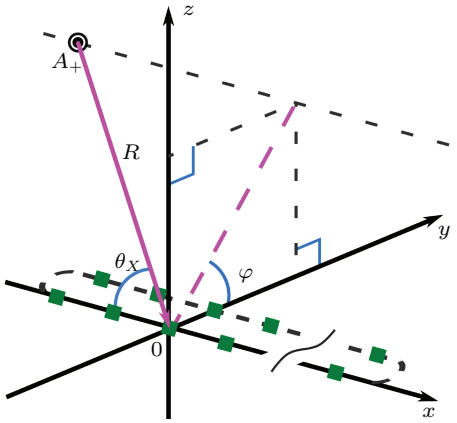


Fig. 3. Angles of incidence of the incoming sound wave on the fish body.

If the sound wavelength is larger than $2a$, then $b_X = d_X$ and

$$\begin{aligned}
f_\omega(\boldsymbol{d},\boldsymbol{b}) = -\frac{1}{2}&\left[\gamma_{11}(q\cos\theta_X,q)+\gamma_{12}(q\cos\theta_X,q)\,\mathrm{e}^{-\mathrm{i}q(\boldsymbol{d}\cdot\boldsymbol{g})}\right. \\
&+\gamma_{21}(q\cos\theta_X,q)\,\mathrm{e}^{\mathrm{i}q(\boldsymbol{d}\cdot\boldsymbol{g})} \\
&\left.+\gamma_{22}(q\cos\theta_X,q)\right]\delta(\cos\theta_X-\cos\vartheta_X).
\end{aligned} \tag{26}$$

Thus, for sound wavelengths greater than $2a$, that is, if the condition (14) holds, sound scattering will occur while maintaining the projection of the wave vector on the direction parallel to the lateral line. Given the conservation of this component of the wave vector, the scattering amplitude in the plane perpendicular to the lateral line as a function of $q=\frac{\omega}{c}$, angle θ_X and the scattering angle ϕ in the plane perpendicular to the lateral line,

$$\phi=\cos^{-1}\left(\frac{(\boldsymbol{d}\cdot\boldsymbol{b})-\cos^2\theta_X}{\sin^2\theta_X}\right),$$

is determined by the expressions

$$\begin{aligned}
f_\omega(\vartheta_X,\phi) &= -\frac{1}{2}\cdot\frac{2D(q\cos\theta_X,q)-\mathrm{e}^{-\mathrm{i}q(\boldsymbol{d}\cdot\boldsymbol{g})}Q(q\cos\theta_X,q)-\mathrm{e}^{\mathrm{i}q(\boldsymbol{d}\cdot\boldsymbol{g})}Q(-q\cos\theta_X,q)}{D^2(q\cos\theta_X,q)-Q(q\cos\theta_X,q)\,Q(-q\cos\theta_X,q)}, \\
D(q\cos\theta_X,q) &= \ln\left(\frac{\mathrm{e}^{-\beta a}}{2\,|\cos qa-\cos(qa\cos\theta_X)|}\right)-\mathrm{i}\pi,\quad Q(q\cos\theta_X,q)=\sum_n\frac{\exp[\mathrm{i}q\,|n\boldsymbol{a}-\boldsymbol{g}|+\mathrm{i}q\cos\theta_X na]}{|n\boldsymbol{a}-\boldsymbol{g}|}.
\end{aligned} \tag{27}$$

These expressions can be further simplified, given that the x-component of the vector $\boldsymbol{g}$ is negligibly small or can be neglected

due to other reasons (for example, if $a \ll |\boldsymbol{g}|$ and $qa \ll 1$). In such cases due to the equality $Q(k,s) = Q(-k,s)$ the expression (27) takes the form

$$f_\omega(\vartheta_X,\phi) = -\frac{D(q\cos\theta_X,q) - \cos(\boldsymbol{q}\cdot\boldsymbol{g})Q(q\cos\theta_X,q)}{D^2(q\cos\theta_X,q) - Q^2(q\cos\theta_X,q)}$$
$$= -\frac{1}{2}\left[\frac{1-\cos(\boldsymbol{q}\cdot\boldsymbol{g})}{D(q\cos\theta_X,q) - Q(q\cos\theta_X,q)} + \frac{1+\cos(\boldsymbol{q}\cdot\boldsymbol{g})}{D(q\cos\theta_X,q) + Q(q\cos\theta_X,q)}\right]. \tag{28}$$

4. Discussion

The starting point for the development of the considered model was the mechanism of a sound detection by the lateral line of fishes proposed in Refs. [20,21], where the corresponding analysis was generally qualitative. In the present paper we develop a quantitative approach, which allows to distinguish the pressures caused by an external source on the lateral lines on the different sides of the fish body trunk and to calculate the differential cross section of sound scattering on the lateral line.

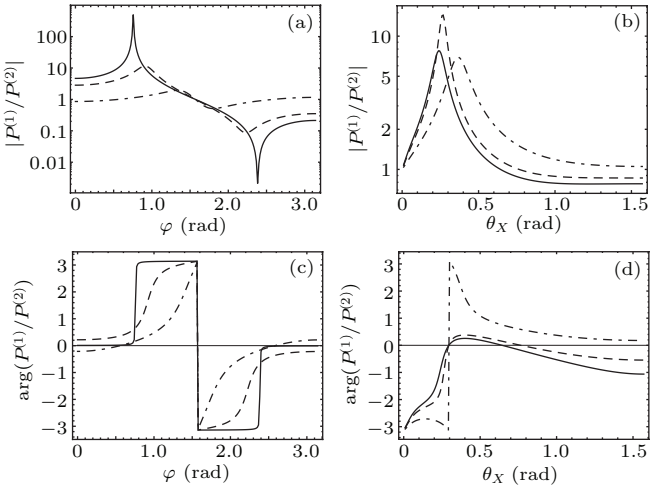


Fig. 4. The ratio of the pressure amplitudes and the phase difference for pressures $P^{(1)}(t), P^{(2)}(t)$ on the flanks of the fish, calculated by formula (17) for the frequency corresponding to $qa = \pi/6$: (a) $\left|\frac{P^{(1)}(t)}{P^{(2)}(t)}\right|$ as a function of φ for different values of θ_X; (b) $\left|\frac{P^{(1)}(t)}{P^{(2)}(t)}\right|$ as a function of θ_X for different values of φ; (c) $\arg\left(\frac{P^{(1)}(t)}{P^{(2)}(t)}\right)$ as a function of φ for different values of θ_X; (d) $\arg\left(\frac{P^{(1)}(t)}{P^{(2)}(t)}\right)$ as a function of θ_X for different values of φ. In images (a) and (c), solid, dashed and dash-dotted lines correspond to $\theta_X = \frac{\pi}{10.6}, \frac{\pi}{9}, \frac{\pi}{4}$, respectively. In images (b) and (d), solid, dashed and dash-dotted lines correspond to $\varphi = 0, \frac{\pi}{6}, \frac{\pi}{3}$, respectively.

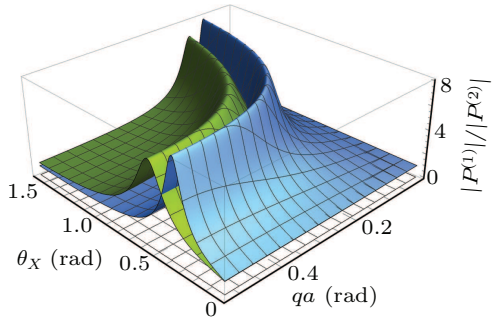


Fig. 5. The ratio $\left|\frac{P^{(1)}(t)}{P^{(2)}(t)}\right|$ for different qa and θ_X ($\varphi = 0$ (blue) and $\varphi = \frac{\pi}{3}$ (green)).

The expressions obtained for the excess pressures on the lateral line on opposite flanks of the fish caused by a remote point source demonstrate a pronounced dependence of those pressures both on the sound frequency and source position relative to the fish body in terms of the angles θ_X and ϕ (see Figs. 4 and 5).

Dependence on the angles becomes stronger with increasing sound frequency and manifests itself strongly for the phase shift and amplitudes quotient for fluctuations of excess pressures on both sides of the lateral line along sides of the fish.

In the case of sound scattering on a lateral line within the framework of the considered model, the projections of wave vectors of the incident and scattered sound waves onto the lateral line, as expected from symmetry considerations, are preserved. Note that in this case the dependence of the scattering amplitude on angles θ_X and ϕ becomes more pronounced with the increasing frequency (Fig. 6).

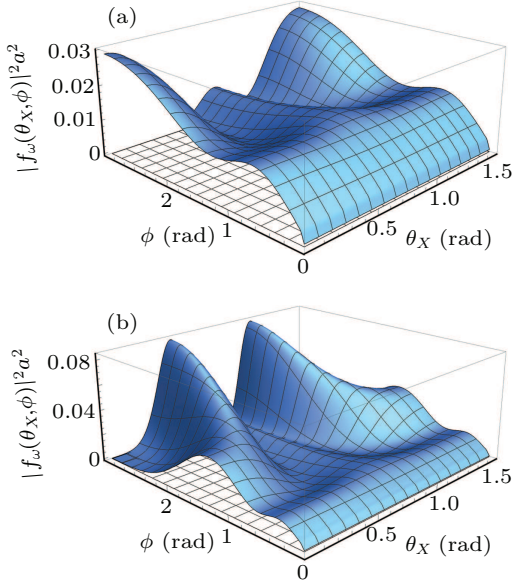


Fig. 6. The differential scattering cross section $|f_\omega(\theta_X,\phi)|^2$ calculated by formula (28) for the frequency of the sound wave corresponding to $qa = \frac{\pi}{12}$ (a) and $qa = \frac{\pi}{6}$ (b).

Of course, due to the excessive sketchiness of the proposed model and insignificant simplifications in the calculations, the results obtained do not reveal the entire functionality of the lateral line of fishes. However, the model can be improved. Instead of point potentials, one can use resonators with a point window approximation (see Refs. [30,31]) or point potentials with an internal structure.[36] For fishes

with lateral lines of the "surface" type, Green's function for free space might be replaced by Green's function for two half-spaces with different speeds of sound,[37,38] and for fishes with lateral lines of the "cannel type", i.e., by Green's function for three-dimensional space with a potential with periodic internal structure, concentrated on two parallel lines. All these changes make it possible to expand the scope of the model under consideration. However, these improvements are unlikely to substantially change the pronounced binaural effect (see Figs. 4 and 5), which, in our opinion, allow fishes to determine the bearing of sound sources.

Note that even in the present form the model and its results can be useful for the rapidly developing field of the development and application of an artificial later line and different later-line-inspired sensors.[39,40] Such sensors find their use in aeroacoustic measurements,[41] hydrodynamic sensing,[42–45] as a navigational instrument for robotic fishes,[46–49] etc.

Acknowledgements

This work was supported by the Ministry of Education and Science of Ukraine (Grant No. 0115U003208). The authors thank Dr. R. Fricke for useful advice.

References

[1] Popper A N, Hawkins A D, Sand O and Sisneros J A 2019 *J. Acoust. Soc. Am.* **146** 948
[2] Coffin A B, Zeddies D G, Fay R R *et al.* 2014 *J. Exp. Biol.* **217** 2078
[3] Dijkgraaf S 1962 *Biol. Rev.* **38** 51
[4] Webb J F 2011 *Encyclopedia of fish physiology: from genome to environment* 1st edn (London: Academic Press) pp. 336–346
[5] Jiang Y, Ma Z and Zhang D 2019 *Bioinspir. Biomim.* **14** 041001
[6] Maruska K P 2001 *The behavior and sensory biology of elasmobranch fishes: An anthology in memory of Donald Richard Nelson* (Berlin: Springer) pp. 47–75
[7] Zeddies D G, Fay R R and Sisneros J A 2011 *Encyclopedia of fish physiology: From genome to environment* 1st edn (London: Academic Press) pp. 298–303
[8] Yoshizawa M, Jeffery W R, van Netten S M and McHenry M G 2014 *J. Exp. Biol.* **217** 886
[9] Jiang Y, Fu J, Zhang D and Zhao Y 2016 *J. Bion. Engin.* **13** 108
[10] Hawkins A D and Popper A N 2018 *J. Acoust. Soc. Am.* **144** 3329
[11] Cardinal E A, Radford C A, Mensinger A F 2018 *J. Exp. Biol.* **221** jeb180679
[12] Denton E J, Gray J A B and Blaxter J H S 1976 *J. Mar. Biol. Assoc. UK* **59** 27
[13] Finneran J J and Hastings M C 2000 *J. Acous. Soc. Am.* **108** 1308
[14] Kalmijn A J 1988 *Sensory biology of animals* (New York: Springer-Verlag) p. 131
[15] Mann D A, Lu Z and Popper A N 1997 *Nature* **389** 341
[16] Carpenter K E, Berra T M and Humphries Jr. J M 2004 *J. Morphol.* **260** 193
[17] Ramcharitar J U, Deng X, Ketten D and Popper A N 2004 *J. Comparative Neurol.* **475** 531
[18] Lychakov D V and Rebane Y T 2000 *Hear Res.* **143** 83
[19] Schuijf A and Buwalda R J A 1975 *J. Comparative Physiol. A* **98** 333
[20] Popov I Y and Popova S L 1995 *Biophysics* **40** 443
[21] Popov I Y and Popova S L 1997 *Italian J. Pure Appl. Math.* **20** 83
[22] Albeverio S, Gesztesy F, Hoegh-Krohn R and Holden H, with an appendix by Exner P 2005 *Solvable models in quantum mechanics* 2nd edn (Providence R.I.: AMS Chelsea Publishing)
[23] Van Netten S M 2006 *Biol. Cybern.* **94** 67
[24] Goulet J, Engelmann J, Chagnaud B P *et al.* 2008 *J. Comp. Physiol. A* **194** 1
[25] Mogdans J and Bleckmann H 2012 *Biol. Cybern* **106** 627
[26] Ristroph L, Liao J C and Zhang J 2015 *Phys. Rev. Lett.* **114** 018102
[27] Herzog H, Klein B and Ziegler A 2017 *J. R. Soc. Interface* **14** 20160898
[28] Oteiza P, Odstrcil I, Lauder G *et al.* 2017 *Nature* **547** 445
[29] Brasche J, Exner P and Kuperin Yu A and Seba P 1994 *J. Math. Anal. Appl.* **184** 112
[30] Popov I Y 1992 *Math. USSR-Sbornik* **71** 209
[31] Popov I Y 1992 *J. Math. Phys.* **33** 3794
[32] Popov I Y and Popova S L 1993 *Europhys. Lett.* **24** 373
[33] Popov I Y and Popova S L 1993 *Phys. Lett. A* **173** 484
[34] Blaxter J H S 1987 *Biol. Rev.* **62** 471
[35] Mantile A, Posilicano A and Sini M 2016 *J. Different. Equ.* **261** 1
[36] Pavlov B S 1987 *Russian Math. Surveys* **42** 127
[37] Popov I Y, Adamyan V M, Blinova I V and Popov A I 2015 *Nanosystems: Phys. Chem. Math.* **6** 611
[38] Adamyan V M, Popov I Y and Blinova I V 2016 *Electron. J. Theor. Phys.* **13** 173
[39] Liu G, Wang A, Wang X and Liu P 2016 *Appl. Bion. Biomech.* **2016** 4732703
[40] Zhai Y, Zheng X and Xie G 2021 *J. Bion. Engin.* **18** 264
[41] Merino-Martinez R, Sijtsma P, Snellen M *et al.* 2019 *CEAS Aeronaut. J.* **10** 197
[42] Chen N N, Tucker C, Engel J M, Yang Y C, Pandya S and Liu C 2007 *J. Microelectromech. Sys.* **16** 999
[43] Shu Y, Tian H, Wang Z *et al.* 2015 *Chin. Phys. Lett.* **32** 114301
[44] Jiang Y G, Ma Z Q, Fu J C and Zhang D Y 2017 *Sensors* **17** 1220
[45] Liu G J, Liu S K, Wang S R, Hao H H and Wang M M 2019 *J. Bion. Engin.* **16** 1007
[46] Liu G J, Gao S X, Sarkodie-Gyan T and Li Z X 2018 *Measur. Sci. Technol.* **29** 125102
[47] Zheng X, Wang C, Fan R and Xie G 2018 *Bioinspir. Biomim.* **13** 016002
[48] Tang Z J, Wang Z, Lu J Q, Ma G Q and Zhang P F 2019 *Electronics* **8** 566
[49] Sharif M A and Tan X 2019 *Bioinspir. Biomim.* **14** 055003